Chapter 3 Design and Simulation Results

3-1 Omnidirectional Reflector

The principal application of photonic crystal is to confine the propagation of light. Thus, the 1-D photonic crystal is almost used for substituting the mirrors of a resonator. Comparing with metallic mirrors, 1-D PC has the advantage of the frequency selectivity and extremely low loss, so it's very useful for the construction of a high-quality closed resonator, such as stadium-like resonator.

In section 2-2.3, we illustrated that the omnidirectional reflection from a 1-D PC can be realized, consequently, the *omnidirectional reflector* can be designed. The omnidirectional reflection bandwidth, i.e., the width of the omnidirectional bandgap, is dominated by the index contrast of the two layers, n_1/n_2. For an isotropic infinite multilayer stack, the index contrast for omnidirectional reflection should be greater than 1.5 [19]. In our case, the index contrast of two materials TiO_2/SiO_2 chosen is about *1.6*, so the omnidirectional reflection bandwidth is very narrow. We can see the bandwidth list in Table 3-1.

d_1/d_2	0.5	0.6	0.65	0.7	0.8	0.85
bandgap range	0.318 ~ 0.323	0.308 ~ 0.317	0.305 ~ 0.313	0.302 ~ 0.312	0.297 ~ 0.306	0.293 ~ 0.302
bandgap width	0.00549	0.0088	0.00871	0.00968	0.00947	0.00889

Table 3-1 The frequency range and bandwidth of omnidirectional bandgap.

All of the data are the normalized frequency, in unit *c*/*D*.

These data are calculated form the band structure mentioned in section 2-2.2. The values of range and width are both shown in normalized frequency. After the refractive indices of two layers being fixed, the band structure is determined only by thickness contrast of two layers of a unit cell. However, in the table we notice that the variation is limited. If we want to widen the bandwidth, we have to do it in another way. The most important and well known method for enlarging bandwidth is to form a heterostructure, which is the combination of two different structures [20].

In most of past researches the 1-D PC structure is the *quarter-wave stack*; whose thickness of each layer is equal to the quarter wavelength of the wave in each layer, i.e., the thickness contrast d_1/d_2 is equal to n_2/n_1. In our case, n_1=2.36 and n_2=1.47, so the thickness contrast of the quarter-wave stack is about 0.62. In table 3.1, it is obvious that the quarter-wave stack isn't the best choice. The optimal ratio of thickness is 0.7.

Therefore, we combine three multilayers, and each of them has ten periods of two layers whose index contrast d_1/d_2 is 0.7. The lattice constants of these three PCs are 0.1744μm, 0.1689μm, and 0.1635μm, individually. In order to observe the result of this design, we calculate the transmission spectra by transfer matrix method. Because the band width of omnidirectional reflection is dominated by the bandgap of the TM-polarization side of band structure (see Fig. 2-2.), we only calculate the transmission spectra of the TM-polarized wave and show them in Fig. 3-1.

In Fig. 3-1, we can see that the expected overlap between bandgap of two transmission curves indeed exists for $\theta=0^o$ and $\theta=80^o$. The central frequency of the bandgap gradually shift higher with the larger incidence angle of light (This phenomenon can be predicted by observing band structure), so the overlap bandgap of $\theta=0^o$ and $\theta=80^o$ is certainly equal to the omnidirectional reflection band. These two figures in Fig. 3-1 show the wavelength ranges of the transmission less than 0.05 are

0.539~0.55μm and 0.529~0.57μm, respectively. We obtained *3.4* times omnidirectional reflection bandwidth by using heterostructure.

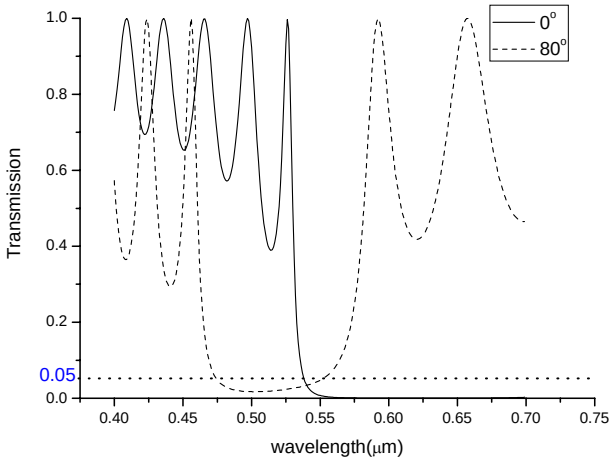

Fig. 3-1 (a)
The transmission spectra calculated for single multilayer.

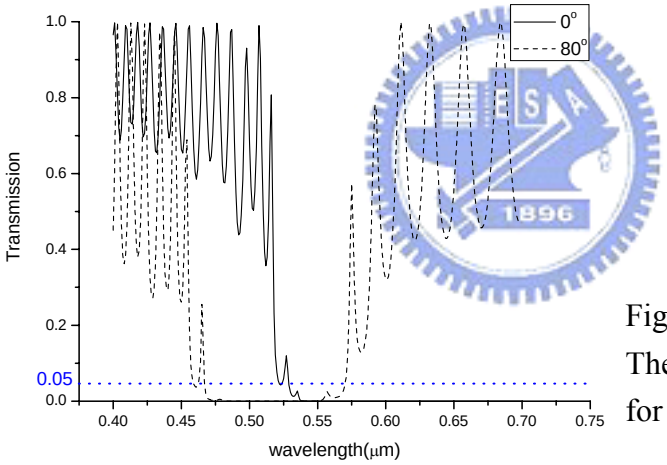

Fig. 3-1 (b)
The transmission spectra calculated for heterostructure.

3-2 Omnidirectional Dichroic Beam Splitter

3-2.1 Motivation

Almost all of the omnidirectional 1-D photonic crystals are used for design of the omnidirectional reflector in use of the omnidirectional photonic bandgap. However, photonic crystals still have the characteristic of allowed band. To apply this property, we try to design a dichroic beam splitter, which can split two beams of light at different frequencies with one being reflected and the other being transmitted. General dichroic beam splitter are produced for working at the incidence angle $\theta=45^{o}$. We will design a dichroic beam splitter which has large working range of incidence angle. Our research will concentrate on 1.3μm/1.55μm beam splitter because it is useful for optical communication and WDM.

3-2.2 Initial concept and simulation results

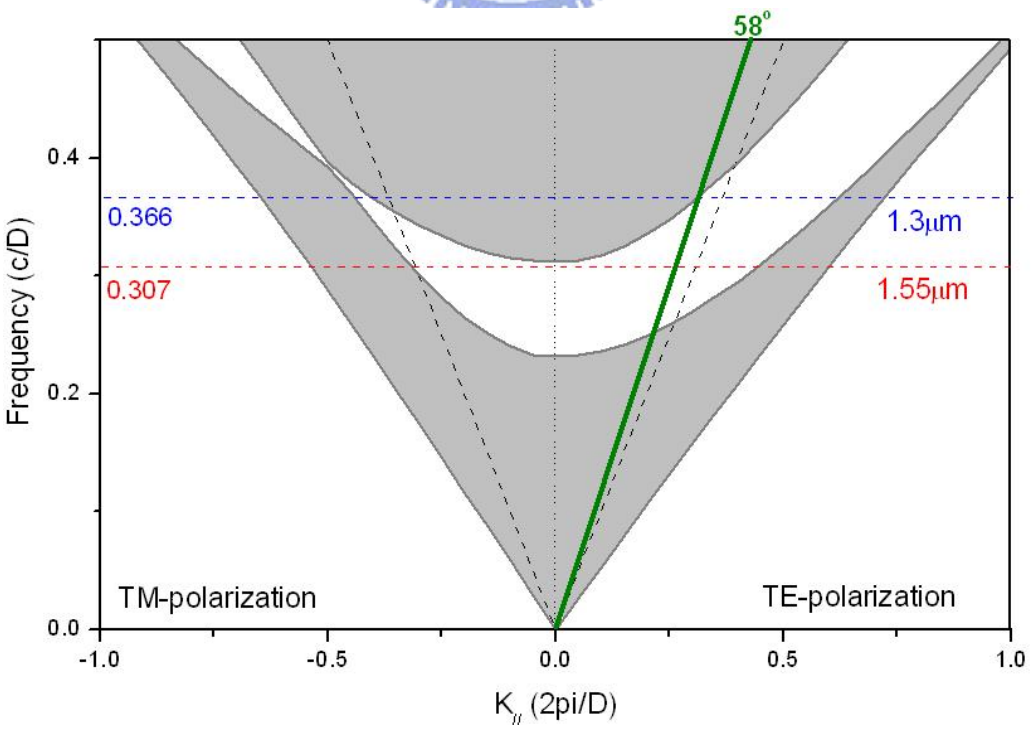

Fig. 3-2 Band structure ($d_1/d_2=0.7$) calculated by plane wave expansion method.

We choose the band structure of d_1/d_2=0.7 in Fig. 3-2. By choosing the proper lattice constant, we can locate 1.3μm wavelength in the allowed band and 1.55μm within the omnidirectional bandgap. Thus, the light beam of 1.3μm will pass through this multilayer and that of 1.55μm will be reflected. This lattice constant is 0.4758μm.

In Fig. 3-2 we can see that the normalized frequency of 1.3μm isn't completely located in the allowed band inside the line cone. The TE-polarized light beam of 1.3μm will be reflected when the incidence angle is larger than 58°. We calculate the transmission diagram of this design (10 periods) by transfer matrix method. The angular transmission is shown in Fig. 3-2-2.

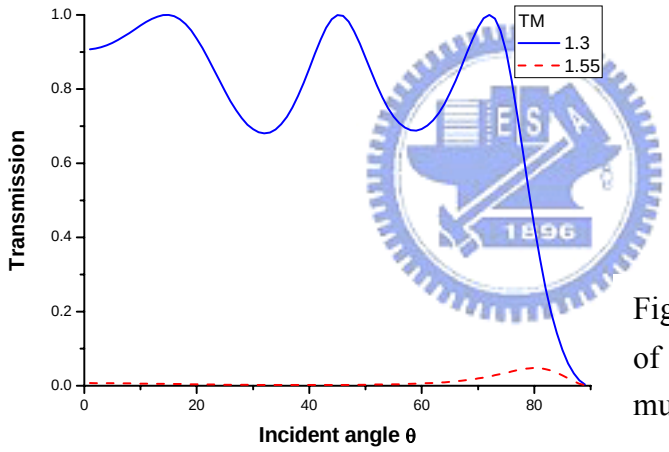

Fig. 3-2-2 (a) Transmission diagram of TM-polarized incident wave. This multilayer has 10 periods.

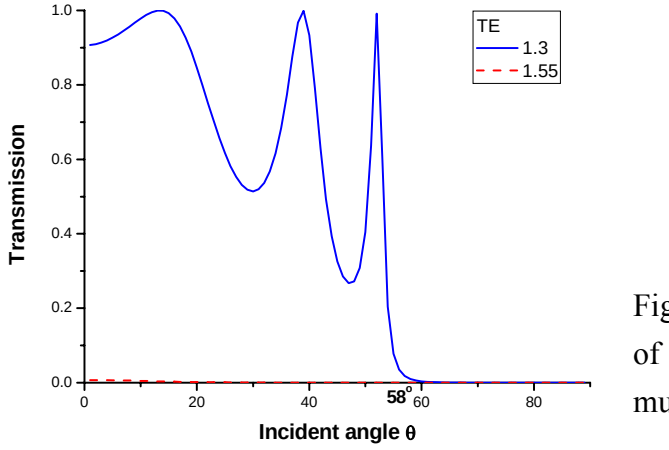

Fig. 3-2-2 (b) Transmission diagram of TE-polarized incident wave. This multilayer has 10 periods.

The transmission of 1.55μm incident wave of both polarizations approach to zero (less than 0.05) within whole range of incidence angle. Disregarding the serious transmission ripple in TE-polarization, the transmission of 1.3μm wave is almost 1 and reduces to zero for $\theta>58^{o}$. Therefore, the designed dichroic beam splitter works quite well within $\theta<58^{o}$ if the ripples were removed. In the next section, we will try to develop a method to broaden the working range of incidence angle.

3-2.3 Method to design an omnidirectional dichroic beam splitter

In order to enlarge the allowed range of incidence angle, or even to achieve omnidirection, we start from realizing the band structure. As the incidence angle of TE-polarized wave is increased, the bandwidth of bandgap becomes larger. However, due to small frequency ratio of 1.3μm and 1.55μm the separation of these two frequencies is too narrow to cover the bandgap at large angle. After trying with different d_1/d_2, we still cannot find proper band structure to avoid this problem.

Therefore, it is necessary to introduce some particular structures to overcome the obstacle. We recall that the method mentioned in section 3.1, the combination of multilayers, used to broaden the frequency range, may be useful to broaden the range of incidence angle as well.

The principle of using heterostructure is to extend the forbidden band, i.e., the bandgap, not the allowed band. Therefore, we must revise the lattice constant to make the normalized frequency line (in band structure) of 1.3μm TE-polarized wave entirely located in allowed band within light cone. While we shift the normalized frequency of 1.3μm wave to the position above the intersection point of light line and the edge of second band, parts of the normalized frequency of 1.55μm is moved to allowed band (see Fig. 3-3(a)). Accordingly, the second multilayer is made for

insulating the incident 1.55μm wave within incidence angle θ<58°. In Fig. 3-3(b), we can see the normalized frequency of 1.3μm will fall in the bandgap if we try to block the incident 1.55μm wave within θ<58°. Surely we have tried the other band structures and never found suitable heterostructures.

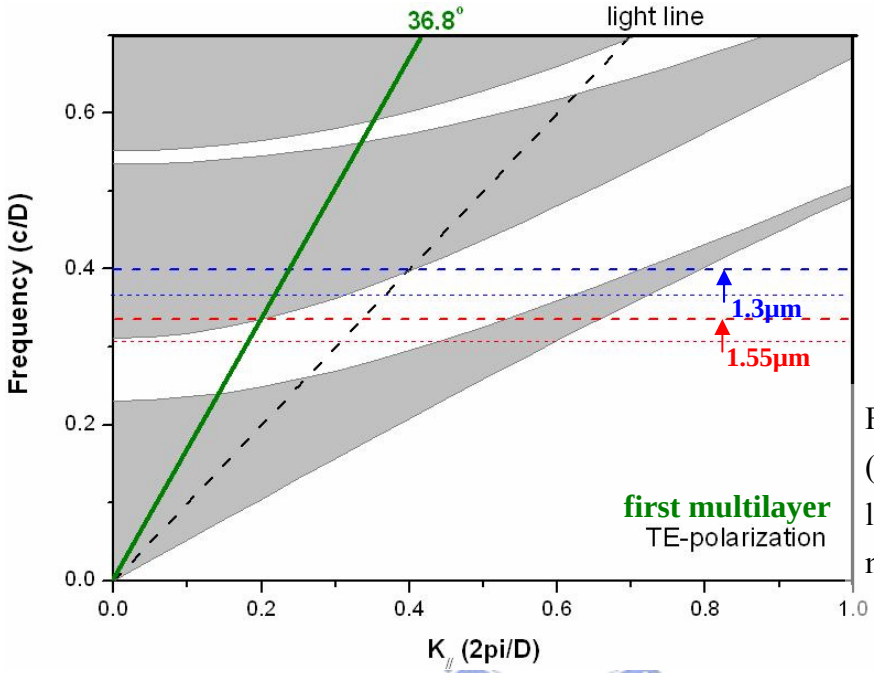

Fig. 3-3 (a) Band structure (d_1/d_2=0.7) and the choice of lattice constant of the first multilayer of heterostructure.

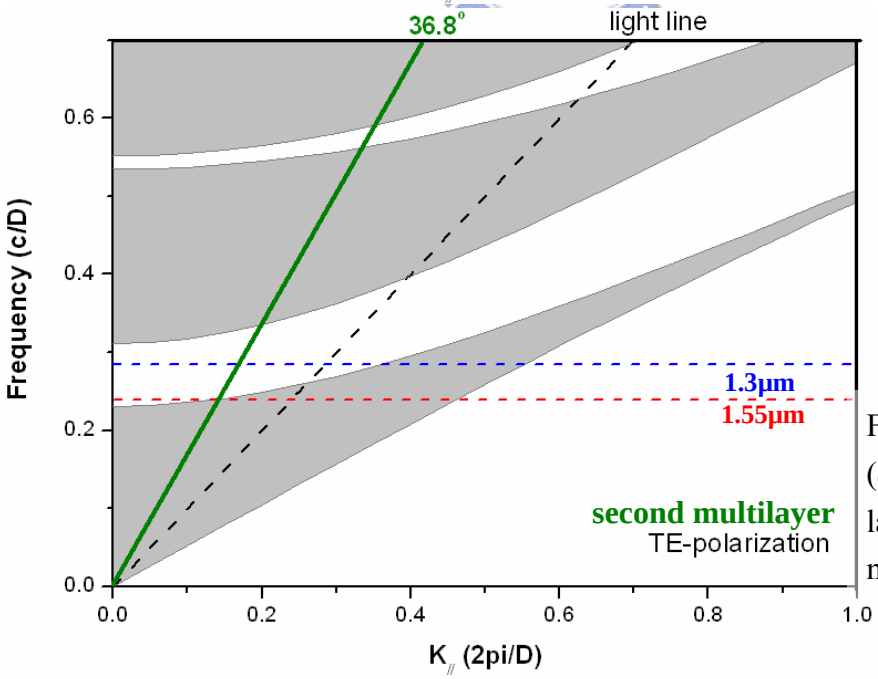

Fig. 3-3 (b) Band structure (d_1/d_2=0.7) and the choice of lattice constant of the second multilayer of heterostructure.

Most of research is focusing on the first bandgap of 1-D photonic crystal, but

we notice that the second bandgap has some special characteristic. Compared with the first bandgap, the second one is narrower and flatter, so it is beneficial for us to separate two frequencies. In Fig. 3-4(b), we see the design of the second multilayer and some problems. The normalized frequency of 1.3μm cannot locate completely in allowed band inside the light cone, and of 1.55μm still have leaky band pass from this heterostructure between θ=27.8^{o} and θ=36.8^{o}.

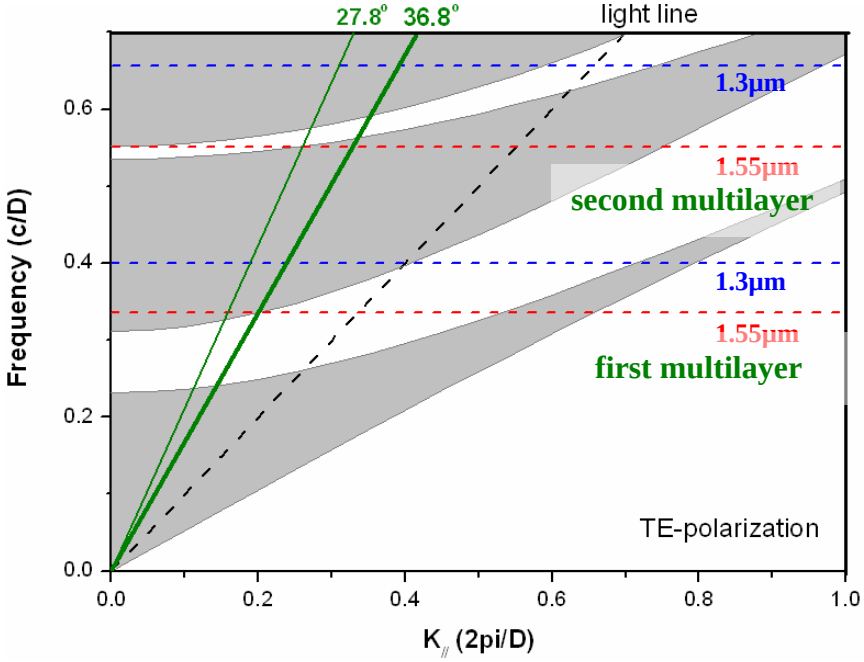

Fig. 3-4 Band structure and the selection of two lattice constants of the heterostructure

The method of using heterostructure seems unworkable, so an omnidirectional dichroic beam splitter seems impossible. However, we will propose that it could be realized and the heterostructure is useful. A new structure will be introduced to accomplish the design in the next section.

3-2.4 One more layer for each unit cell

In order to achieve our anticipation, the common used structure for multilayer

coating technology, the dielectric multilayer structure of alternating layers of high and low refractive index, must be modified. Here we propose the *three-layer unit cell* structure, i.e., the multilayer whose unit cell is composed of three dielectric slabs. This additional layer we choose is ZrO_2, whose refractive index n_3 is *2.19*. The band structure calculated from this unit cell is shown in Fig. 3-5

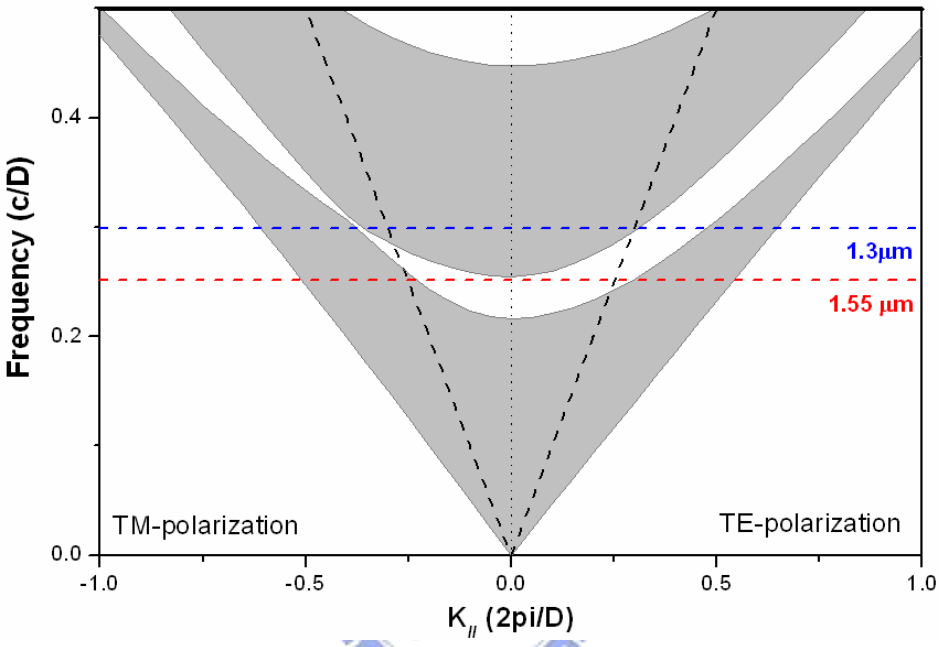

Fig. 3-5 Band structure calculated form three-layer unit cell where n_1=2.36, n_3=2.19, n_2=1.47 and d_1:d_3:d_2=2:1:1. The choice of lattice constant D (d_1+ d_2+ d_3) is *0.39μm* for this two frequencies we set.

In Fig. 3-5 we can see this structure do not have the omnidirectional bandgap. On the contrary, this narrow bandgap is advantageous for our design. The normalized frequency of 1.3μm and 1.55μm locates on entire allowed band and the center of bandgap (no omnidirection), respectively. Although parts of TM-polarized 1.55μm wave enter the allowed band at large incidence angle, we still can block this transmission by using heterostructure; it is easy to finish in this structure. In Fig. 3-6, the appropriate frequency selection of two multilayers is plotted. In order to insulate the band pass of 1.55μm incident wave by the first multilayer from θ=67° to θ=90°

(light line), the normalized frequency of 1.55μm we choose by the second multilayer is shifted up (see Fig. 3-6). Therefore, the 1.55μm incident wave from each incidence angle is blocked by this heterostructure and the 1.3μm wave is entirely safe on allowed band (see the two blue lines in Fig. 3-6). The omnidirectional dichroic beam splitter is designed successfully. The lattice constants of two multilayers are 0.39μm and 0.4185μm.

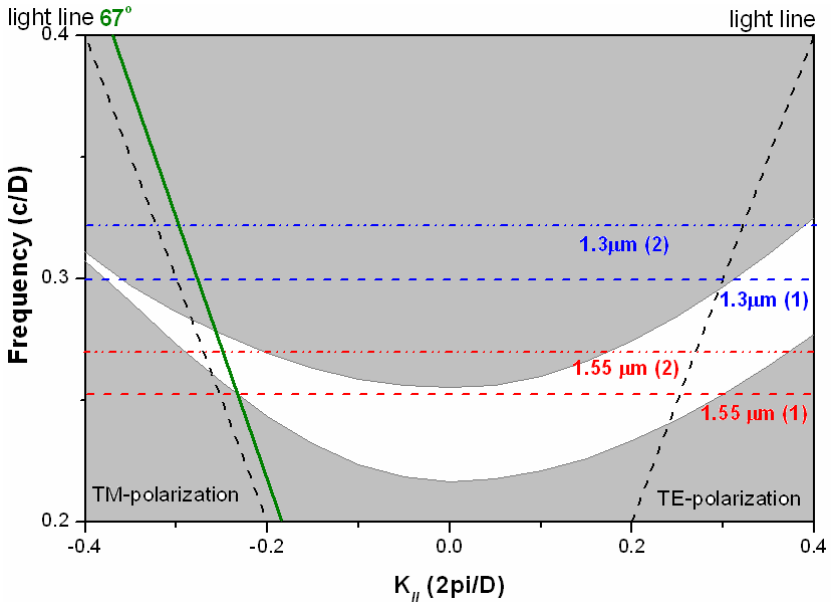

Fig. 3-6 Band structure and the frequency selection for heterostructure. The number in parenthesis means the corresponding multilayer. Lattice constant of first multilayer is 0.39μm, and of second multilayer is 0.4185μm.

And then, we simulate the results of our design in Fig. 3-7. The transmission of 1.3μm TM wave is perfectly high within $\theta=75^{o}$, and disregarding the ripples, that of 1.3μm TE wave also reach 100% within $\theta=80^{o}$. And then, the transmission of 1.55μm wave with both polarizations from each incidence angle is less than 0.07.

Therefore, we extend operation range of incidence angle to approach 80^{o}. An omnidirectional dichroic beam splitter has already been designed in our methods.

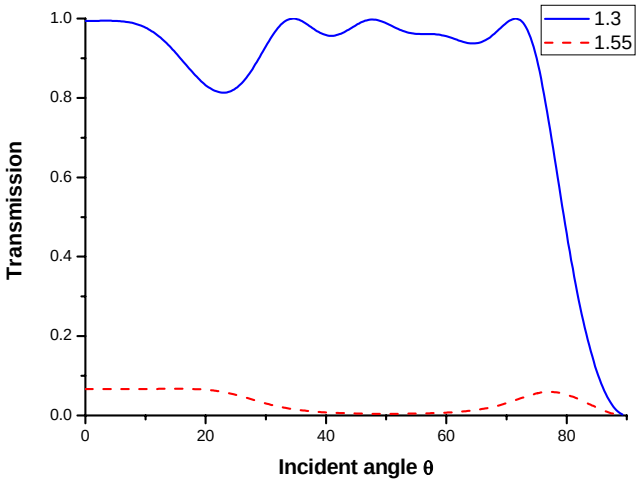

Fig. 3-7(a) Transmission diagram of *TM* wave. It is simulated from the heterostructure, and each unit cell of both multilayers has three layers.

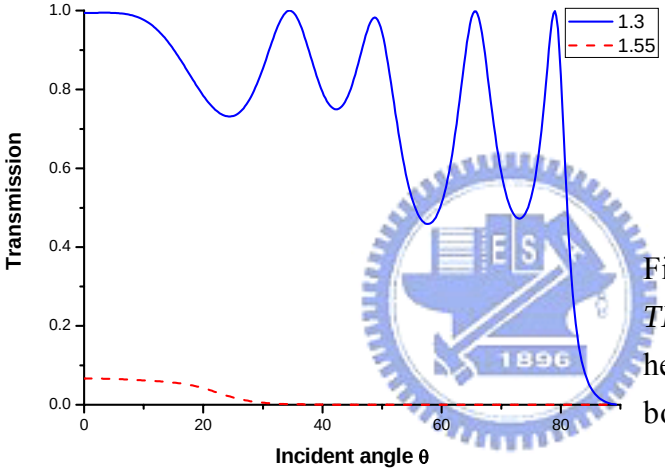

Fig. 3-7(b) Transmission diagram of *TE* wave. It is simulated from the heterostructure, and each unit cell of both multilayers has three layers.

In fact, the dichroic beam splitter (BS) is the most used for splitting two incident light beams at incidence angle $\theta=45^{o}$. If we want a dichroic beam splitter operating for some special incidence angles, we only need to produce another one for this purpose. It seems unnecessary to try designing an omnidirectional BS for all possible use. However, our research has its own value. It can be used as a *tunable* beam splitter; the direction of reflected light beam can be tuned to three or more ports (in our case, 10^{o}, 35^{o}, 50^{o}, and 65^{o} are good choices.). Such designs of tunable beam splitter make more possibility of many new optical systems and devices.

3-2.5 impedance-matching layer

In this section, we try to reduce the ripple effect in the allow band. By adding a quarter-wave-thick layer between PC and air to be an anti-reflection layer (Fig. 3-8), we expect the transmission could be raised [21]. In the other hand, this layer must make the impedance between air and PC match. The refractive index of the layer must satisfy the condition: $n_m = \sqrt{n_{eff} \cdot n_{air}}$.

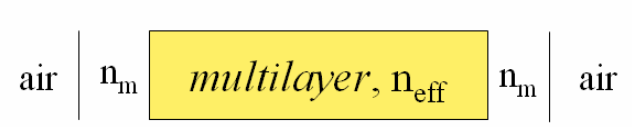

Fig. 3-8 Impedance-matching coating between the 1-D PC and air.

We take the effective index of refraction (n_{eff}) of the multilayer $n_{eff} = (n_1 d_1 + n_2 d_2 + n_3 d_3)/D = 2.1$. Therefore, we calculate the transmission spectra at θ=0°, θ=20°, and θ=50° as Fig. 3-9 for the refractive index and thickness of the impedance-matching layer of 1.45 and 0.224μm. It is obvious that the transmission in allowed band has been raised without changing the bandgap. Note that there is no difference between TE and TM polarization for θ=0°.

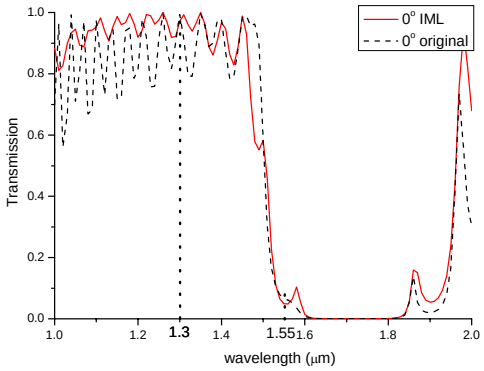

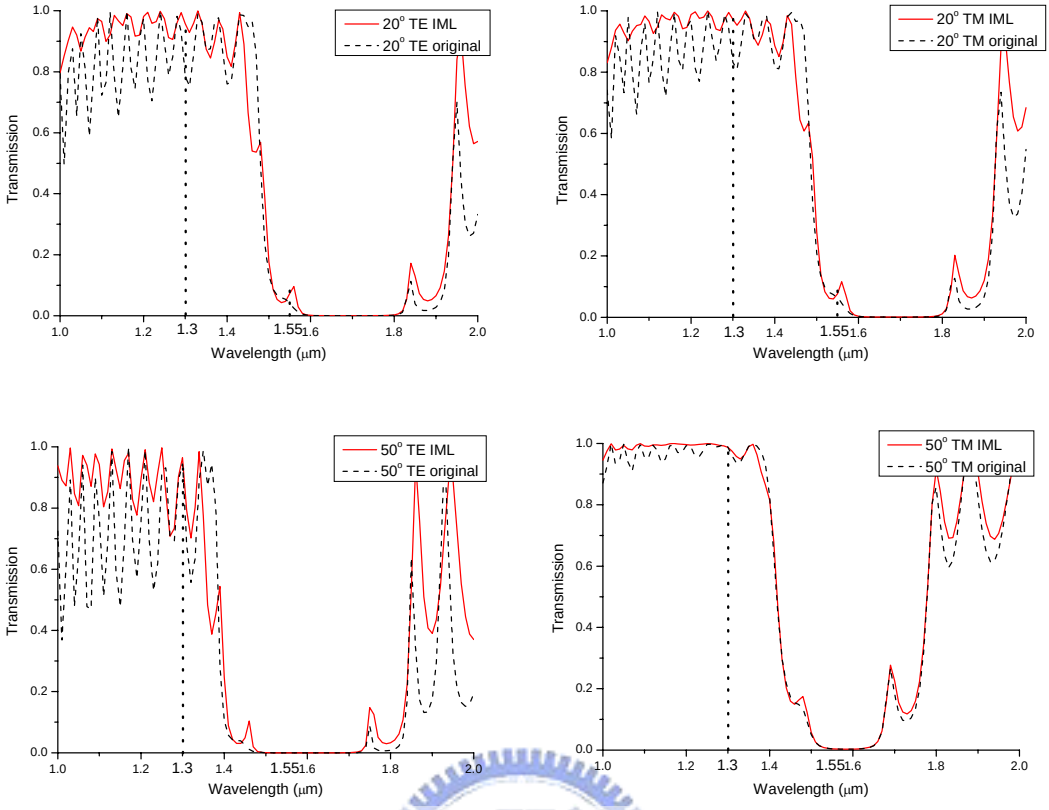

Fig. 3-9 The transmission spectra at θ=0°, θ=20°, θ=50°. Impedance-matching layers (IML) make the transmission in allowed band higher.

However, the transmission as a function of incident angle (in Fig. 3-10) shows flat at small incident angle but still large ripples at large incident angle for TE polarization. We find that the beam splitter will be invalid at large incident angle.

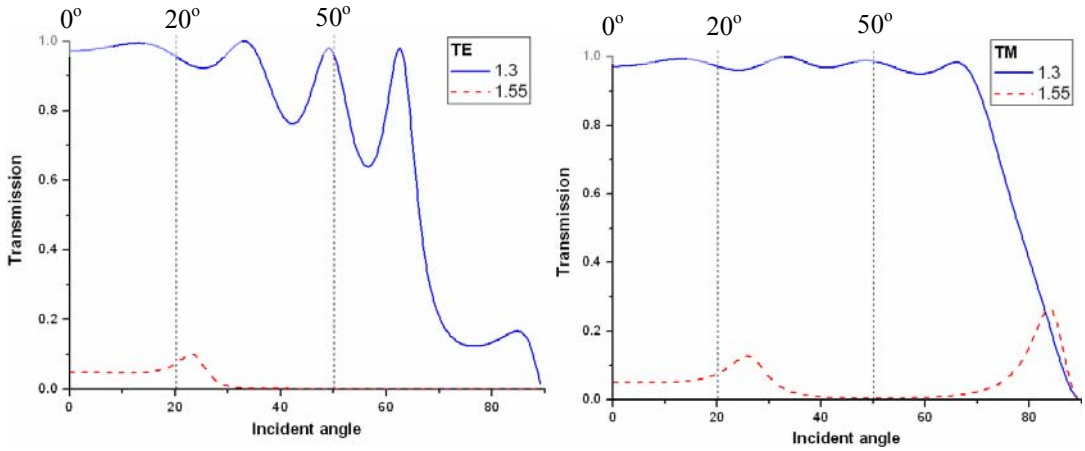

Fig. 3-10 The transmission diagram T(θ) of the multilayer with impedance-matching layer whose thickness is 0.224μm.

The reason for this result may be that the quarter-wave thickness is considered for normal incidence. In order to obtain better result, we can just tune the thickness of the layers. Good performance could be found when it is 0.65μm (see Fig. 3-10-2). We can see the transmission of 1.3μm wave becomes much higher within $\theta<30^{o}$ and the BS still works at large incident angle. Besides, the transmission of 1.55μm wave is also raised. Therefore, in chapter four, we will try to eliminate the ripples by another method.

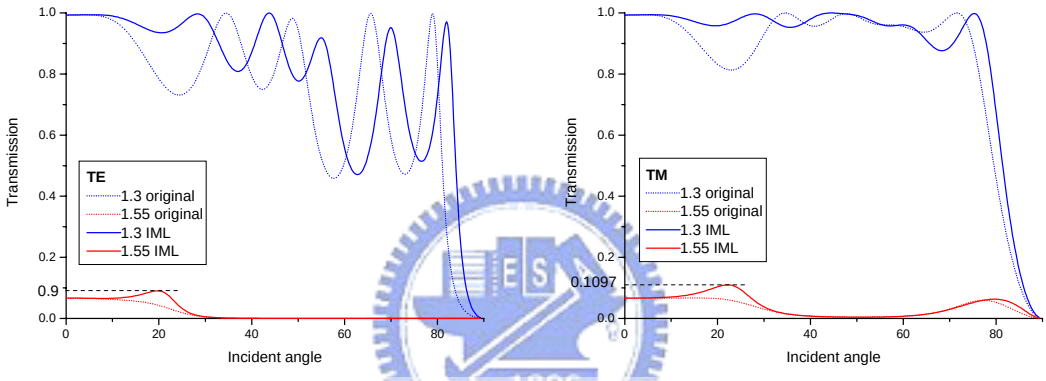

Fig. 3-10-2 The transmission diagram T(θ) of the multilayer with impedance-matching layer whose thickness is 0.65μm.

3-3 Angular tuning Optical Switch

3-3.1 Motivation

In section 3-1, we design the reflector which can isolate the light incident from any incident angle within a frequency range. In section 3-2, we further design a beam splitter, which not only make one frequency isolated but also ensure another frequency passing from any direction. In this section, we consider one frequency could be controlled passing or not. In fact, our initial motivation comes from Fig. 3-2(b). We show this figure again below.

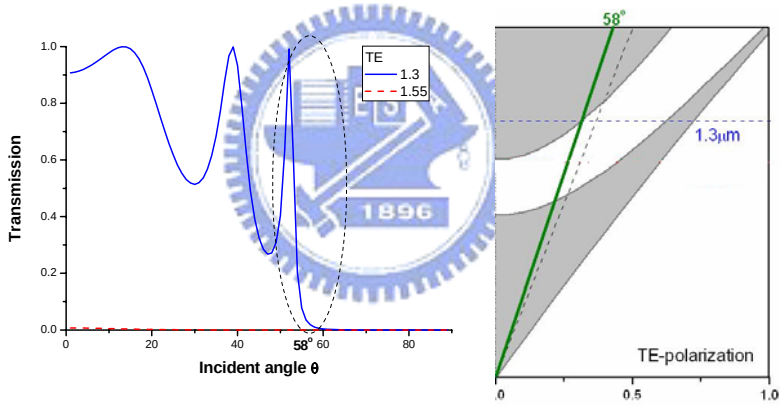

Fig. 3-11 Transmission diagram and corresponding normalized frequency in band structure.

We notice the transmission decline very sharply when the frequency in band structure falls in the bandgap at $\theta=58^{o}$. This simulation result is calculated from only ten periods. Thus, the 1-D photonic crystal may be applied to design an *optical switch*. We will present our model and research in the next section.

3-3.2 Ideal model and design step

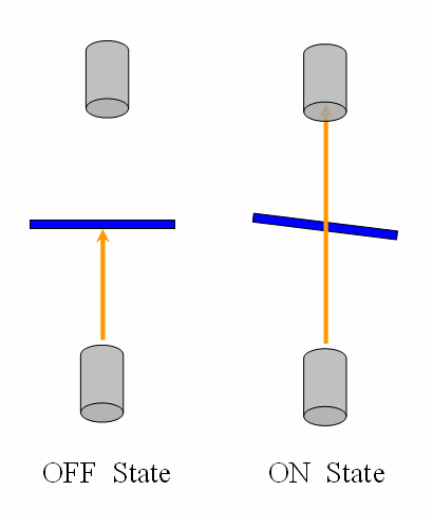

Fig. 3-12(a) First case of our ideal designs.

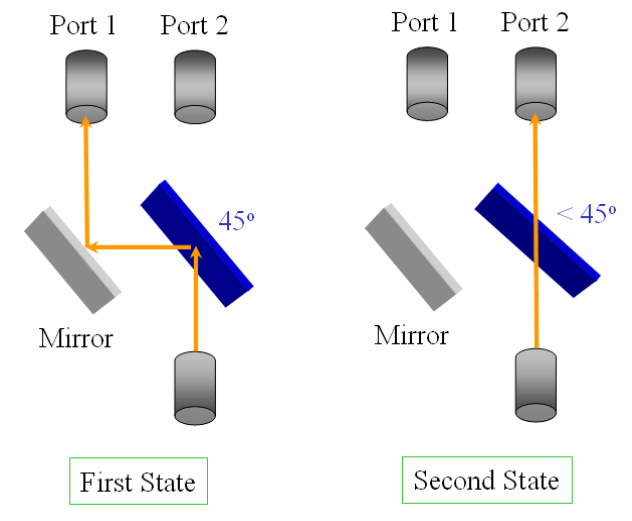

Fig. 3-12(b) Second case of our ideal designs. There is one mirror needed.

Fig. 3-12 shows two ideal designs of optical switches; in the first case, the optical switch operates at $\theta=0^{o}$. When the multilayer is perpendicular to incident light, the light will be reflected, that is in the OFF state. After rotating at a specific angle, the multilayer will permit the incident light to pass and it is in the ON state. Otherwise, we can consider the second case in Fig. 3-12(b). There are two ports to receive the light. By tuning the angle of the multilayer, we can determine the light to enter the port 1 or the port 2. Therefore, to design such optical switches we must make the frequency of incident light locate on proper position in band structure. That is, in case one the frequency will be put inside the bandgap at $\theta=0^{o}$, and in case two it will enter to the allowed band for $\theta < 45^{o}$.

In Fig. 3-13 the two frequency selections are shown. We choose the frequency crossing the first allowed band at $\theta=10^{o}$ in case 1, and falling into the second bandgap at $\theta=45^{o}$ in case 2. We calculate the transmission diagram of ten periods as usual in Fig. 3-14. It is obvious that the transmission of both two cases do not decay sharply. At $\theta=10^{o}$ in the first case and $\theta=45^{o}$ in the second case, the transmission should be high and low respectively, but it isn't. The reason is that the band trend of TE and TM

wave isn't the same, so the frequency selections of TE and TM have to meet halfway. Besides, the most principal cause of this simulation result is that the boundary between allowed band and bandgap may be indistinct, i.e., at the band boundary there could be a little disagreement by using plane wave expansion method for infinite PC instead of finite size.

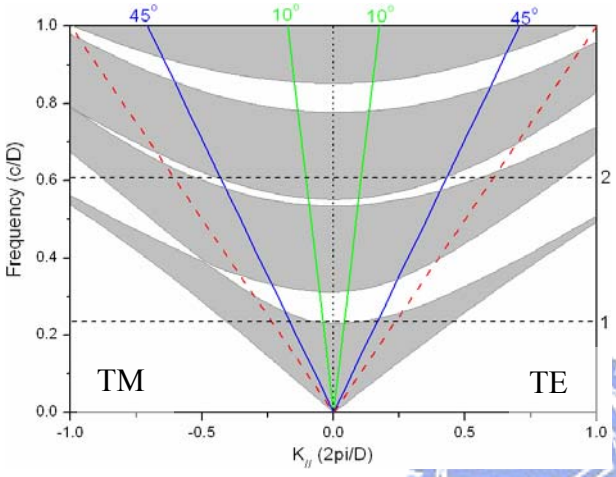

Fig. 3-13 Band structure calculated from d_1/d_2=0.7. Two horizontal dash lines are the frequency for two cases. The red dash lines are light lines.

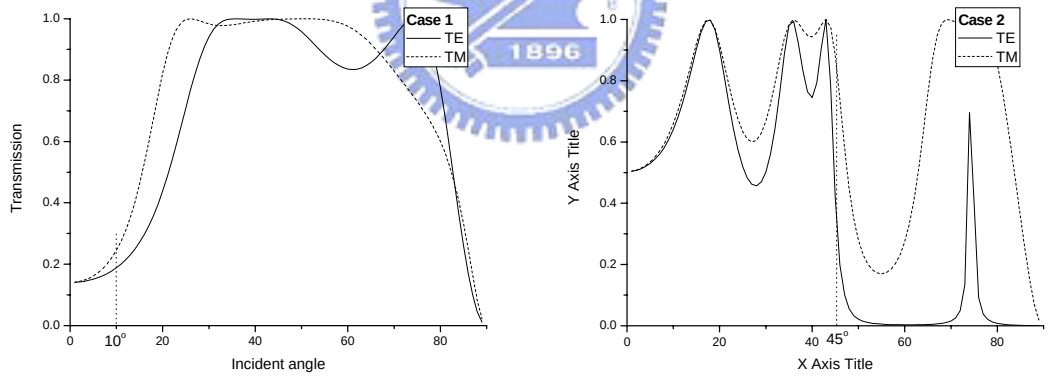

Fig. 3-14 The transmission diagram of two cases calculated from ten periods.

We calculate the transmission of a multilayer of twenty periods and show in Fig. 3-14-2. The transmission curves become sharper and lower at bandgap. But they still don't satisfy our anticipation at $\theta=10^o$ in the first case and $\theta=45^o$ in the second case. Besides, if the transmission curves of TE and TM waves can not only match to each other but also become flatter (i.e., few ripples) in the allowed band, it will work better

for optical switches

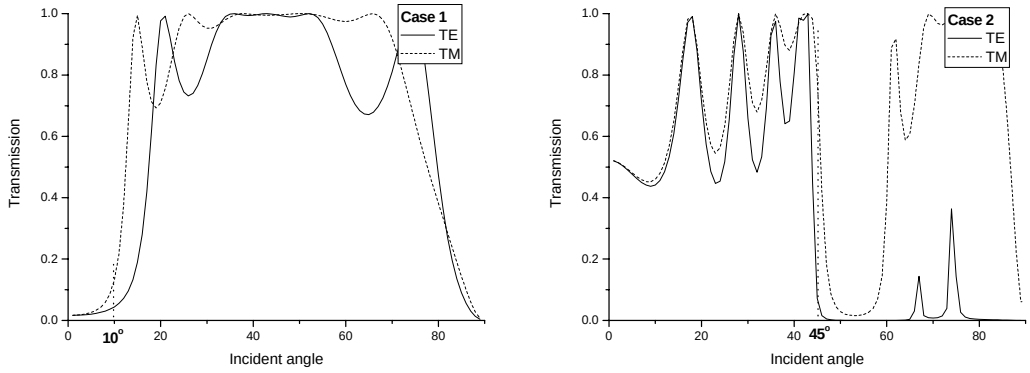

Fig. 3-14-2 The transmission diagram of two cases calculated from twenty periods.

3-3.3 Results

After patiently searching for a good performance of the optical switch, we find a better result in use of the same band structure of d_1/d_2=0.7 as shown in Fig. 3-15. The chosen normalized frequency is 0.866. The simulation result is shown in Fig. 3-15 (b). We can see the transmission curve is perfectly flat in the allowed band for both TE and TM waves and perfectly match to each other within the working range. The reason we use the fourth allowed and the third bandgap is that the trend of bandgap and allowed band become symmetrical. Thus, the transmission of ten-period layers for TE wave at $\theta=10^o$ and $\theta=20^o$ are 0.93 and 0.02, and these for TM wave are 0.96 and 0.05, respectively.

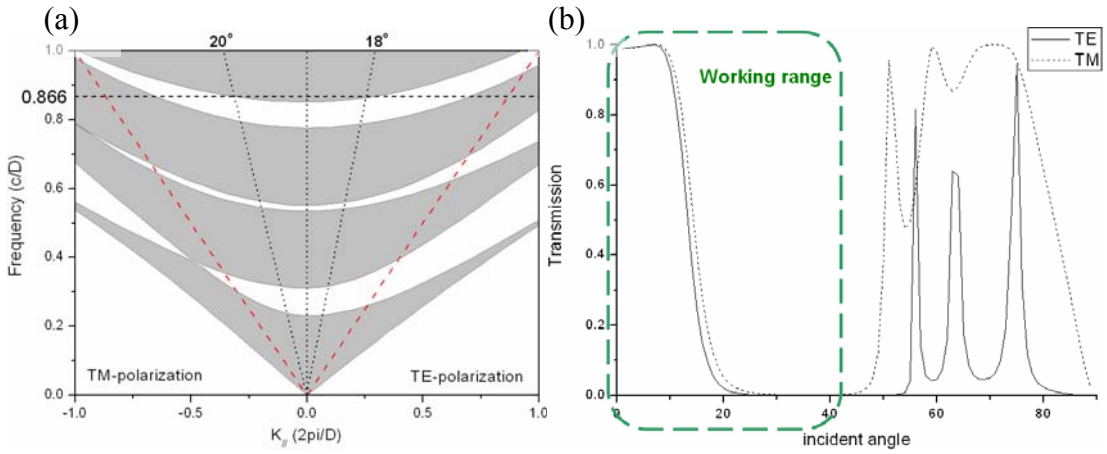

Fig. 3-15 (a) The band structure (d_1/d_2=0.7) and frequency selection (Ω=0.866). (b) The corresponding transmission diagram and perfect range for optical switch use.

It's a pity that this performance isn't fit for our ideal designs in using angle, and maybe the curve can decline more sharply. If we want to search better results, random trying is time-consuming. The unwanted ripples in the allowed band are always unpredictable in band structure. "When one door shuts another door opens", in the next chapter, we will propose the characteristic band structure for efficiently designing omnidirectional photonic devices with fewer ripples.